Environment Canada
Environnement Canada

National Water Research Institute
Institut National de Recherche sur les Eaux

AN INSTRUMENT FOR MEASURING FRAZIL CONCENTRATION

By

Gee Tsang

Inland Waters Directorate
Direction Générale des Eaux Intérieures

Tsang(49)

Study 83-316

This manuscript has been submitted to the Journal of Cold Regions Science and Technology for possible publication and the contents are subject to change

AN INSTRUMENT FOR MEASURING FRAZIL CONCENTRATION

By

Gee Tsang

Environmental Hydraulics Section
National Water Research Institute
Canada Centre for Inland Waters
Burlington, Ontario, Canada L7R 4A6

January 1984

ABSTRACT

This paper reports the development and calibration of an instrument that can measure the point concentration of frazil in water. The instrument is constructed on the physical principle of comparative resistance measurement. Laboratory testing of the instrument showed that the instrument worked satisfactorily. The measured concentration by the instrument was found to be greater than the theoretical concentration calculated from heat balance measurements by a factor F, called the calibration factor. F is the product of two parts; the corrective coefficient because of the anistropy of the frazil crystals F_r and the turbulence corrective coefficient C_t associated with the sluggishness of the frazil flocs in passing through the sensor probe. F_r, called the real calibration factor of the instrument, was found to be approximately equal to 2.2. The value of C_t was found to be approximately unity at a high flow velocity of 21.4 cm/s and in the range of 1.6-1.8 at a flow velocity of 15-16 cm/s. The value of C_t under other flow and turbulence conditions can be obtained through calibration.

RÉSUMÉ

Dans le présent article, on traite de la mise au point et de l'étalonnage d'un instrument permettant de mesurer en un point donné la concentration du frasil dans l'eau. Cet instrument est construit d'après le principe physique de la mesure comparative des résistances. L'essai en laboratoire de l'instrument a montré que celui-ci fonctionnait de façon satisfaisante. On a constaté que la concentration mesurée par l'instrument était supérieure à la concentration théorique calculée d'après les mesures du bilan thermique, d'un facteur F, appelé facteur d'étalonnage. F est le produit de deux éléments; le coefficient correctif Fr, dû à l'anisotropie des cristaux de frasil, et le coefficient correctif Ct, dû à la turbulence qui résulte de la lenteur des flocs de frasil à passer par la microsonde. On a constaté que Fr, appelé facteur d'étalonnage vrai de l'instrument, était approximativement égal à 2,2. On a constaté que Ct était approximativement égal à l'unité pour une vitesse élevée d'écoulement, soit 21,4 cms, et de l'ordre de 1,6 à 1,8 pour une vitesse d'écoulement de 15 à 16 cm/s. On peut obtenir par étalonnage la valeur de Ct dans d'autres conditions d'écoulement et de turbulence.

MANAGEMENT PERSPECTIVE

This report describes the operation of a prototype instrument which will provide a means to measure the quantity of frazil ice present in flowing water.

Before the development, there was no quantitative measurement of frazil ice in motion. The instrument will provide new information important to the research aimed at understanding and predicting frazil in flowing water.

Such information and theories are significant where there are concerns for northern river development, power production into basin transfer of water and for the assessment of the impact of winter navigation in channels and rivers. A private company ARCTEC is already endeavouring to construct an operational version of this prototype for use in fresh and salt water. The latter broadens the usefulness to arctic and cold water studies for energy developments.

T. Milne Dick
Chief
Hydraulics Division

PERSPECTIVES DE GESTION

Dans le présent rapport, on décrit le fonctionnement d'un prototype d'appareil qui permettra de mesurer la quantité de frasil présente dans l'eau en mouvement.

Avant la mise au point de cet appareil, il n'était pas possible de mesurer quantitativement le frasil en mouvement. L'instrument en question fournira de nouvelles informations importantes pour la recherche visant à mieux expliquer et prédire les concentrations de frasil dans l'eau en écoulement.

Ces informations et théories seront importantes pour étudier les effets de l'aménagement des cours d'eau dans le Grand Nord, la production d'hydroélectricité, et l'évaluation de l'incidence de la navigation hivernale dans les chenaux et cours d'eau. La compagnie privée ARCTEC cherche déjà à construire une version opérationnelle de ce prototype, qui soit utilisable en eau fraîche et en eau salée. Ce prototype élargit le champ d'application des études sur les eaux froides et arctiques, consacrées aux utilisations de l'énergie.

Le chef de la Division de l'hydraulique
T. Milne Dick

1.0 INTRODUCTION

In turbulent water, the ice formed is in the form of fine crystals suspended in the water and is known as frazil. Depending on the degree of supercooling and the salinity of the water, the crystallographic shape and evolution of the frazil are different (Tsang, 1983; Tsang and Hanley, 1983). For fresh water under most natural conditions, however, the frazil is in the form of discoids that grow into dendritic crystals (Tsang, 1982a).

Frazil can greatly affect the characteristics of the flow. It can also adhere to underwater objects to form anchor ice. In both cases, the conveyance capacity of a water course can be substantially reduced (Ontario Hydro, 1969; Foulds and Wigle, 1977; Tsang, 1982b). When frazil adheres to submerged water intake structures, it often can completely block off the water intake and cause water supply or power production problems (Giffen, 1973). In order to best utilize the water resources during the winter months, the properties and effects to water flow of frazil should be thoroughly studied.

The quantitative study of frazil in the past, however, has been slow. This was largely due to the lack of an instrument that can quantitatively measure frazil. Before embarking on a major effort in frazil research, the development of such an instrument is imperative.

Natural water is electrically conductive because of mineral contents. As the water changes from liquid to solid, however, the impurities are rejected because the orderly arrangement of the ice molecules prohibits the inclusion of other molecules in the lattice structure. Ice crystals themselves, therefore, are electrically non-conductive. Thus, by measuring the electrical resistance of a water-frazil mixture, the amount of frazil in the mixture may be evaluated. Kristinsson (1970) probably was the first person to construct an instrument using the above principle to measure frazil in a river. He wound two wires spirally on an insulator rod and immersed the rod in the river. By measuring the resistance between the two wires, the

concentraton of frazil over the depth of the rod was estimated. Also using the same principle but by measuring the increased conductivity of the water because of salt rejection, Giffillian et al (1972) were able to calculate the amount of ice formed in a river. Besides the electrical conductivity principle, frazil may also be measured with an instrument constructed on the calorific principle as contemplated by Ford (1982), among others, or on the laser doppler principle, as reported by Schmidt and Glover (1975). A working instrument based on the latter two principles, however, has not been produced thus far.

The conceptual design and the theoretical ground work guiding the design of an instrument based on the conductivity principle for measuring the point concentration of frazil, the velocity of the frazil packs and the velocity of the flowing water was proposed by Tsang (1973). An experimental instrument was later constructed which verified the soundness of the frazil sensing principle (Tsang, 1977). Further development of the instrument following the experimental instrument culminated in the working instrument reported in this paper. This instrument was intended for laboratory use and could measure instantaneously the concentration of frazil in flowing water at a point. Slight modification and reinforcement of the instrument should make it adaptable for field use. By using two instruments simultaneously at two points along a streamline, one may measure the velocity of frazil packs of various sizes.

2.0 THEORY

Because frazil is electrically non-conductive, its concentration in water can be measured by comparing the resistance of a sample of frazil-free water with that of a sample of frazil laden water.

In Fig. 1, the resistance between the pair of electrodes is given by

$$R = D/A \qquad (1)$$

where ρ is the resistivity of the water, D is the length of the electrical path or the separation of the plates and A is the area receiving the electrical lines or the surface area of one electrode plate.

The resistivity (or conductivity) of the water is determined by the number of ions in it and the state of agitation of the ions. Because the former is determined by the salt content of the water S and the latter is controlled by the temperature of the water T, the resistivity of the water should be a function of the following form:

$$\rho = f(S,T) \tag{2}$$

Salt content is defined as the mass of salts per unit volume of solution. In a water body where frazil is continuously formed (and the ice is excluded from the water sample), because of the rejection of salts by the ice, the salt content of the water increases continuously and is given by

$$S = \frac{M_s}{V_o - V_f} \tag{3}$$

where V_o is the total volume of the frazil/water body, V_f is the volume of frazil and M_s is the mass of the salts dissolved in the water part of the mixture.

The above equation may be rearranged to give

$$S = \frac{M_s/V_o}{1 - V_f/V_o} = \frac{S_i}{1 - \bar{c}_f} \tag{4}$$

where $S_i = M_s/V_o$ is the initial salt content of the water before frazil is formed and $\bar{c}_f = V_f/V_o$ is the average volumetric concentration of frazil in the frazil/water mixture.

Because the conductivity of the water is proportional to the number of ions in it or to the salt content of the water and resistivity is the reciprocal of conductivity, one may write

$$\rho_i(T) = \text{Const.}/S_i \quad \text{and} \quad \rho(T) = \text{Const.}/S \tag{5}$$

where T indicates the given temperature and the subsrcipt i indicates the initial condition before frazil is formed. From Eqs. 4 and 5, one has

$$\rho(T) = (1 - \bar{c}_f)\, \rho_i(T) \tag{6}$$

and the substitution of the above equation into Eq. 1 gives

$$R(T) = (1 - \bar{c}_f)\, \rho_i(T)\, D/A \tag{7}$$

The above equation states that the resistance between the plates in Fig. 1 is affected by the temperature of the water and the average concentration of frazil in the water.

Although the electrodes may be of any geometric shape, for easy comprehension and mathematical manipulation, they are assumed here to be rectangular with sides L_2 and L_3 and L_1 apart. Calling the probe for which the water sample is frazil-free the reference probe and the probe for which the water sample is frazil laden the sensor probe, then for the reference probe, the electrical path length will be L_1 and the area receiving the electrical lines will be L_2L_3. The resistance between the two plates of the reference probe thus will be

$$R_r(T) = (1 - \bar{c}_f)\, \rho_i(T)\, L_1/(L_2L_3) \tag{8}$$

where the subscript r refers to the reference probe.

For the sensor probe, the electrical path will be longer than $L_\perp$ because the electrical lines have to go around the frazil crystals on their way from one electrode to the other. If the sample volume between the electrodes is divided into many small tubes spanning from one electrode plate to the other with a cross-sectional area equal to the average size of the frazil crystals and the distribution of the frazil crystals is assumed to be uniform, then for each tube there will be n crystals for the electrical line to go around. Let the representative linear dimension of the frazil crystals be ℓ, the length of the electrical path then will be

$$D = L_\perp + \Delta L_\perp = L_\perp + n\,\xi\ell = L_\perp(1 + n\xi\ell/L_\perp) \qquad (9)$$

where ξ is the shape factor of the frazil crystals and $\Delta L_\perp = n\xi\ell$ is the increase in electrical path length because of frazil presence.

The presence of frazil also affects the electrical line receiving area of the electrode plates. Fig. 2 shows one electrode plate covered with a layer of water of thickness ℓ. If this thin water layer is divided into many vertical and horizontal tubes of width ℓ as shown in Fig. 2, then there will be m crystals per vertical tube and p crystals per horizontal tube and the receiving area of the electrode will be given by

$$A = (L_2 - m\xi\ell)(L_3 - p\xi\ell) = L_2L_3\left(1 - \frac{m\xi\ell}{L_2}\right)\left(1 - \frac{p\xi\ell}{L_3}\right) \qquad (10)$$

In using the same shape factor for the three directions, the geometric shape of the frazil crystals has been assumed isotropic. Because of the uniform distribution assumption, one has

$$n\xi\ell/L_\perp = m\xi\ell/L_2 = p\xi\ell/l_3 = \Delta L/L \qquad (11)$$

The substitution of the above equation into Eqs. 9 and 10 and then the substitution of the latters into Eq. 7 lead to

$$R_s(T) = (1 - \bar{c}_f)\, \rho_i(T)\, \frac{L_1}{L_2 L_3} \left[\frac{1 + \Delta L/L}{(1 - \Delta L/L)^2}\right] \qquad (12)$$

where the subscript s indicates the sensor probe.

The quantity in the square bracket in the above equation can be related to the concentration of frazil in the probe. From volumetic considerations, one sees that the concentration of frazil in the probe is given by

$$c_f = \frac{L_1 L_2 L_3 - (L_1 - n\xi\ell))L_2 - m\xi\ell)(L_3 - p\xi\ell)}{L_1 L_2 L_3} \qquad (13)$$

where the first term of the numerator on the right hand side of the equation is the total sample volume and the second term is the volume of the water without frazil. Because in most practically important cases, the concentration of frazil in water is small, seldom exceeding a few percent, $n\xi\ell$, $m\xi\ell$ and $p\xi\ell$ will be small compared with L_1, L_2 and L_3 respectively. By expanding Eq. 13 and neglecting the higher order terms, one will obtain

$$c_f = n\xi\ell/L_1 + m\xi\ell/L_2 + p\xi\ell/L_3 = 3\Delta L/L \qquad (14)$$

The substitution of the above equation to Eq. 12 leads to

$$R_s(T) = (1 - \bar{c}_f)\, \frac{(1 + c_f/3)}{(1 - c_f/3)^2}\, \frac{\rho_i(T)\, L_1}{L_2 L_3} \qquad (15)$$

It should be carefully noted that the above equation contains two frazil concentrations, $\bar{c}_f$ and c_f. While $\bar{c}_f$ is the average concentration of

frazil of the water body as a whole, c_f is the concentration of frazil in the sensor probe or the concentration of frazil at the sensed point. These two concentrations must not be confused.

$(1 - c_f/3)^2$ in the above equation may also be expanded and the higher order term of $c_f/3$ dropped because of its small magnitude. This will reduce Eq. 15 to

$$R_s(T) = (1 - \bar{c}_f) \frac{(1 + c_f/3)}{(1 - 2c_f/3)} \frac{\rho_i(T)\, L_1}{L_2 L_3} \tag{16}$$

The expression of $1/(1 - 2c_f/3)$ may be further expressed as a series of $2c_f/3$ and the higher order terms of $2c_f/3$ in this series may be once again ignored. Such an exercise will reduce the above equation to

$$R_s(T) = (1 - \bar{c}_f)(1 + c_f/3)(1 + 2c_f/3) \frac{\rho_i(T)\, L_1}{L_2 L_3} \tag{17}$$

The above equation shows that the resistance of the sensor probe not only is affected by the concentration of frazil in the probe, but also affected by the average concentration of frazil in the water body, as well as by the temperature of the water because of its influence on $\rho_i(T)$.

Because the temperature of the water may vary and the average concentration of frazil in the water body is a function of the history of the water body, to evaluate the concentration of frazil at a point by measuring R_s alone will be difficult. This difficulty, however, can be eliminated if instead of measuring R_s, one measures

$$\frac{R_s(T) - R_r(T)}{R_r(T)} \tag{18}$$

The substitution of Eqs. 8 and 17 into the above expression, following the expansion of the multiplication factors and the dropping of the higher order c_f terms, immediately leads to

$$\frac{R_s(T) - R_r(T)}{R_r(T)} = c_f \qquad (19)$$

which is the concentration of frazil in the sensor probe.

Thus, from the above derivation, one sees that by measuring $(R_s - R_r)/R_r$, the concentration of frazil in water can be measured directly. Such a measurement is neither affected by the temperature of the water, nor by the amount of frazil that had formed in the water body. The employment of Eq. 19 for frazil sensing, however, requires that the water in the reference probe and in the sensor probe be of the same temperature, and consequently, be of the same resistivity.

During the derivation of Eq. 19, the straying effect of the electrical lines in the probes has been ignored, the distribution of the frazil crystals has been assumed uniform and the geometric shape of the frazil crystals has been assumed isotropic. The departure of the actual conditions from the above idealizations should affect the final relationship between resistance and frazil concentration. During the derivation, it was also assumed that the concentration of frazil is low. This assumption was one of the conditions leading to the final linear relationship. If this assumption is not observed, one should expect to see a non-linear relationship between $(R_s - R_r)/R_r$ and c_f. However, a one to one relationship between these two variables should still exist.

3.0 DESIGN AND CONSTRUCTION OF INSTRUMENT

According to the theory developed in the preceding section, the conceptual design of the instrument as shown by the block diagram on Fig. 3 was conceived and adopted.

It is seen from Fig. 3 that the design consists of two components, one for frazil sensing and display and the other for deicing control. The frazil sensing and display component is shown by the upper part of the diagram. It is seen from this part of the diagram that the instrument has two probes; the sensor probe for which frazil is present and the reference probe for which frazil is excluded. These two probes are identically constructed and in each probe, an identical A.C. current of constant strength flows between the electrode plates. These two constant A.C. currents are converted from two constant D.C. currents which are generated by two independent constant current sources, one for each probe. The reason to use A.C. currents is to avoid polarization effects which otherwise will produce oxygen and hydrogen bubbles to block the electrode plates. To reduce the electro-chemical effect, the frequency of the A.C. currents is chosen to be high, but not high enough to cause excessive transient effect and unwarranted capacitance leakage. The strength of the currents is also made small, but not too small as to hinder the frazil sensing function of the instrument. The currents in the probes produce a voltage drop of $V_s = R_s I$ across the sensor probe and a voltage drop of $V_r = R_r I$ across the reference probe, I being the strength of the currents. By feeding V_s and V_r to the voltage processor where the voltages are substracted, divided and amplified, one obtains

$$G \frac{V_s - V_r}{V_r} = G \frac{R_s - R_r}{R_r} \tag{20}$$

where G is the dimensional gain factor and is in the unit of voltage. According to Eq. 19, one sees that the above voltage signal is the concentration of frazil in the sensor probe multiplied by the gain factor G.

Three ways are provided to display or to further process the analog signal from the voltage processor. The first is to record the

signal with an external tape recorder for later analysis. The second is to record the signal with a chart recorder that is built in to the instrument and the third is to integrate the signal with an integrator. The reference voltage or the base voltage of the integrator can be varied by means of an external voltage source. This provision enables the integrator to integrate the area between the signal signature and any horizontal line below it (see Fig. 3) and thus provides a way to evaluate the size distribution of the frazil flocs in the flowing water. A counter is connected to the integrator to show the area integrated. The integrator is not intended for online use, but for analysing the signal that had been recorded earlier by the tape recorder and is played back to the instrument.

The bottom part of Fig. 3 shows the deicing component of the instrument. It is seen from the diagram that oil heating is used. Although one may think that electrical heating is a more rational approach, experiences gained during the development of the instrument proved that this is not the case. During the development, electrical heating had been attempted twice and found infeasible because it is expensive to construct, difficult to repair and introduces electrical interference to the frazil signal.

It is seen from Fig. 3 that the electrode plates are embedded in oil vessels in such a way that the back of the plates is exposed to the warm oil and the face of the plates are exposed to the water. Good seal is maintained to ensure that oil will not leak into the water and vice versa. It may be added that the probe supports are also oil heated although this is not explicitly shown in Fig. 3. The temperature of the oil in the probe chambers is controlled by the temperature of the returning oil. When the temperature of the returning oil is measured to be less than the preset value which is above freezing, the heater control will activate the heater in the oil reservoir to heat up the oil. For safety reasons, the temperature of the oil in the reservoir is also sensed. When the oil temperature in the reservoir is higher than

the preset limit, the heater control will cut off the heater as well as the pump to avoid runaway heating.

According to the conceptual design, electronic circuitries and mechanical parts were designed and constructed and a frazil instrument intended for laboratory use as shown by the photograph on Fig. 4 was built.

It is seen from Fig. 4 that the instrument consists of two probes, and oil box and an electronic box. Although the two probes are identically constructed, one should always be used as the sensor probe while the other as the reference probe. The electrodes are 5 cm diameter metal plates and are 5 cm apart, giving a sample volume of approximately 100 cm^3. The metal support of the probes is approximately 1.25 m long. The oil box contains the oil reservoir, the oil pump and the oil temperature sensors. All other electronics are contained in the electronic box. For proprietary reasons, detailed technical information of the instrument may not be revealed in this publication, but may be obtained from the author's affiliated institution through appropriate arrangements.

The overall gain factor of the instrument is G = 51 volts. According to Eq. 20, this means a 0.51 volts output signal will represent a frazil concentration of one percent. The output voltage range of the instrument is 0 - 10 volts, representing a theoretical frazil concentration range of 0 - 19.6 percent.

It was mentioned earlier that the integrator gives the area between the signal curve and the baseline, or

$$\int_\tau (V_{sig} - V_{ref})\, dt \qquad (21)$$

where V_{sig} is the frazil signal voltage of the instrument, V_{ref} is the baseline voltage and τ is the period of integration. Electronics is built in to the instrument to convert the above integration into counts according to

$$N = \frac{1}{0.512} \int_{\tau} (V_{sig} - V_{ref})\, dt \qquad (22)$$

From the above equation, the average value of $(V_{sig} - V_{ref})$ in the time period τ is seen to be given by

$$\overline{(V_{sig} - V_{ref})} = \frac{0.512\ N}{\tau} \qquad (23)$$

4.0 CALIBRATION OF INSTRUMENT

4.1 The Calibration Factor

According to Eqs. 19 and 20, one sees that the measured concentration of frazil in water is given by

$$c_{fm} = V_{sig}/G = V_{sig}/51.0 \qquad (24)$$

where the second subscript m indicates the value is a measured value.

Eq. 19 was derived assuming that the shape of the frazil crystals is isotropic. In reality, this is not the case and frazil crystals can be in the shapes of discoids, needles and flakes, although in most natural cases they are of the discoid shape. Because of the anisotropic shape of the frazil crystals, the electrical lines between the two electrode plates of the sensor probe are longer than those if the frazil crystals were isotropic. The longer electrical lines means that the voltage drop across the sensor probe should be greater than the theoretical value or that the signal output from the instrument should be greater than the theoretical signal output by a multiplying factor greater than unity. Let F be this multiplying factor or calibration factor and c_{ft} be the theoretical frazil concentration, from the above discussion, one sees that

$$F = c_{fm}/c_{ft} \tag{25}$$

The objective of the calibration was to obtain the values of F and to see what factors will affect this calibration factor.

4.2 The Calibration Setup

The instrument was calibrated in a cold room. A recirculating flume as shown in Fig. 5 was constructed to facilitate the calibration. It is seen from Fig. 5 that the flume was race-course shaped and had a cross-section of 15 cm (6") wide and 13 cm (5") deep. During the calibration, it was filled with tap water to 2 cm from the top. The diameter of the probe was of a comparable dimension to the depth of the water, so the measured concentration of frazil may be approximately considered as the concentration of frazil of the water in the flume. A variable speed propeller was mounted at one end of the flume to produce a current of the desired velocity. To cool the water more quickly in the flume, a fan (not shown) was placed about 1.5 m from the flume and which produced a wind of about 0.5 m/s over the water. The temperature of the water was measured with a thermometer that had a resolution of 0.001°C and an accuracy of 0.002°C. The air temperature was measured with a thermometer that was accurate to 0.02°C. To prevent frazil from being nucleated by and adhering to the sides and bottom of the flume, the flume was embedded in a warm air jacket. Light bulbs and recirculating fans were installed in the air jacket to enable the temperature in the air jacket to be adjusted from 2°C to 7°C. It is seen from Fig. 5 that while the sensor probe was placed in the main stream, the reference probe was accommodated in a depression chamber added to the bottom of the flume. The depression chamber was covered with two half-plates with slots cut in them for the probe supports to pass through. Because the depression chamber was surrounded by warm air, the water exchange between the main stream and the chamber was limited by the small slots

in the half-plates and the natural buoyancy of ice discourages frazil from moving down into the depression chamber, the water temperature in the chamber was measured to be at freezing and no frazil was observed in the chamber during the calibration.

The water temperature and the air temperature were recorded on chart. The voltage signal from the frazil instrument was recorded both on chart and on tape for later analysis.

4.3 Experiments and Treatment of Experimental Data

A total of five experiments were conducted for the calibration. The parameters of the experiments are summarized in Table 1. It is seen from Table 1 that three experiments (Tests 1, 2 and 3) were conducted for a slow flow velocity of about 15 cm/s and two experiments (Tests 4 and 5) were conducted for a fast flow velocity of approximately 21.4 cm/s. It should be mentioned that these velocities were measured before frazil was produced in the flume. Following the formation of frazil in the flume, the flow velocity was visibly reduced although the propeller setting was maintained the same. The velocity of the frazil laden flow was not measured because the lack of established technique. For all the experiments except Test 5, frazil was produced in the flume by seeding the water with ice particles scraped from a slab of ice with a saw blade when the water was supercooled to -.030°C. For Test 5, frazil was produced spontaneously before the water temperature reached -.030°C.

The typical experimental result of the calibration experiments is shown by Fig. 6 which was obtained from tracing the early part of the strip chart obtained during Test 2. It is seen from Fig. 6 that the water temperature was recorded on the upper part of the strip chart and the frazil concentration signal was recorded on the lower part of the strip chart. It is seen from Fig. 6 that when the water temperature was well above the freezing point, a slow chart speed of 0.5 mm/s was used. Because the settings in the cold room was maintained the same during

each experiment, a linear cooling of the water is seen from Fig. 6 with a cooling rate of approximately 4.975×10^{-4}°C/s. As the water temperature approached the freezing point, the chart speed was increased to 2 mm/s to produce a more readable chart. Before the water temperature reached -.030°C, no frazil or other form of ice was observed in the water. The frazil recording in Fig. 6 also shows no detection of frazil. At -.030°C, the supercooled water was seeded. Immediatley following seeding, frazil crystals were seen in the flume. The frazil crystals grew and agglomerated into clusters and flocs which became bigger and thicker with time. As soon as frazil was seen in the flume, it was also detected by the instrument as shown by the frazil concentration recording of Fig. 6. The recording also reflects the growth and agglomeration of the frazil crystals and flocs. Every time a floc passed through the sensor probe, a spike was recorded. The thicker the floc, the higher was the spike. The frazil instrument, thus was seen to be working. What remained was to calibrate the instrument.

The theoretical concentration of frazil in water can be calculated from the temperature recording of the frazil producing water. If the ambient environment and the hydrodynamic conditions of the water are maintained the same, then from heat balance considerations, the concentration of frazil in the water at time t can be shown to be (Tsang, 1983)

$$c_{ft} = \frac{1}{0.916 H_L} \left[-c\left(\frac{dT}{dt}\right)_n (t - t_n) + c\,(T - T_n)\right] \qquad (26)$$

Where H_L is the latent heat of fusion of ice, c is the specific heat of water, T is the temperature of the water and the subscript n indicates the instant of seeding. The first term inside the square bracket in the above equation is the heat lost to the ambient environment at time t following seeding and the second term is the heat absorbed by the

water to increase its temperature from T to T_n. The sum of these two quantities is the heat that must be supplied by the ice by liberating its latent heat of fusion. The constant 0.916 is to convert the concentration from weight to volumetric.

According to the above equation, if the slope of the approximating straightline to the pre-seeding cooling curve was used for $(dT/dt)_n$, frazil concentration c_{ft} at different instants could be calculated. The theoretical frazil concentration so calculated for the five calibration experiments is shown in Table 1. For the calculations, the time when the temperature curve intersected T = 0°C was considered as time zero. It is seen from Table 1 (and Fig. 6) that for all the calculations, the time interval between two succeeding calculated concentrations was 50 seconds except between the first point and the second point. The first point was the seeding point at which the concentration should be zero by definition and the second point was usually chosen to be the first intersection of the thicker grid line (marking 10 cm distances) with the temperature curve. The length of the centre line of the calibration flume was about 2 m. In 50 seconds, with a flow velocity of 15.0 cm/s and 21.4 cm/s, the frazil laden water would have flowed through the sensor probe 5.35 and 3.75 times respectively.

To obtain the corresponding measured concentrations to the above calculated concentrations, the frazil voltage signal that had been tape-recorded earlier was played back to the integrator of the instrument. The instrument is constructed to accept such an input. The recorded signal was also fed to a chart recorder which reproduced a frazil concentration recording chart similar to the one shown in Fig. 6. A voltmeter was also connected to the chart recorder in parallel to measure the actual voltage of the frazil signal. It is seen from Fig. 6 that before frazil was produced in the flume, a small baseline voltage was given out by the instrument. Although this baseline voltage could be adjusted to zero, it was not done to permit the observation of the meandering of the baseline which was found to be ±50 mV, representing a theoretical concentration of frazil of ±0.1 percent.

A reference voltage equal to the baseline voltage was then fed to the instrument and the instrument integrated the area between the signal curve and the baseline (see Eq. 21). The integrated area was converted into counts by the counter (see Fig. 3) and the counting signal was fed to the event marker of the chart recorder which marked the counts on the margin of the strip chart.

Fig. 7 is an example of the strip chart reproduced by so processing the tape-recorded signal of Test 2. Since both Fig. 6 and Fig. 7 show the early part of Test 2, they should have the same outward appearance. However, this is not so because:

1. The chart speed of the two recordings was different. While Fig. 6 was recorded at a chart speed of 2 mm/s, the chart speed for Fig. 7 was 5 mm/s.
2. Because the voltage range of the chart recorder (0 - 5 V) and the voltage range of the tape recorder (0 - 10 V) were mismatched, so some of the tape-recorded signal for the later part of the test that would be greater than 5 V would go off the chart. To remedy this situation, the tape-recorded signal voltage was compressed by 50 percent through a transformer or operational amplifier built into the tape recorder before being fed to the chart recorder. Because of this, the amplitude of the recording of Fig. 7 is only 50 percent of that of Fig. 6.
3. The zero positions of the two recordings are different.

From Eqs. 23 and 24, after substituting $(V_{sig} - F_{base})$ for $(V_{sig} - V_{ref})$ in Eq. 23 and $(V_{sig} - V_{base})$ for V_{sig} in Eq. 24 because of the presence of the small baseline voltage V_{base}, one obtains

$$c_{fm} = \frac{0.512\ N}{51\tau} \qquad (27)$$

Allowing for the fact that the signal in Fig. 7 has been compressed to 50 percent so the counts shown on the margin should be doubled to give their original value and expressing c_{fm} in percentage, Eq. 27 is modified to

$$c_{fm} = \frac{1.024\ N}{0.51\ \tau} \approx \frac{2N}{\tau} \qquad (28)$$

According to the above equation, the measured concentration for the periods for which the theoretical concentration has been obtained was calculated. These measured values for all the five calibration experiments are shown in Table 1.

5.0 EXPERIMENTAL RESULTS AND DISCUSSIONS

According to Table 1, the measured concentration c_{fm} was plotted against the theoretical concentration c_{ft} as shown in Fig. 8. It is seen from Fig. 8 that for all the five calibration tests, with the turbulent nature of the flow and the non-uniformity nature of frazil distribution in the flow because of flocking and agglomeration, the relationship between c_{fm} and c_{ft} was surprisingly linear. The slope of the fitted straightlines for the five plots fitted with the method of least squares is shown in Table 2.

It is seen from Table 2 that the slope or the calibration factor of the instrument was affected by the velocity of the flow. However, for a given flow velocity, the calibration factor was not affected by the air temperature which controlled the rate of heat loss from the water or the rate of frazil formation. When the flow velocity was in the 15-16 cm/s range, Tests 1, 2 and 3 showed that the calibration factor varied from 3.560 to 3.885 with a mean of 3.734, giving a deviation from the mean of less than 5 percent. When the flow

velocity was 21.4 cm/s, Tests 4 and 5 showed that the calibration factor was 2.538 and 2.207 respectively. The average value was 2.373 and the deviation of the calibration factor from the mean was less than 7 percent. The decrease of F with the increase of flow velocity was apparent. As the velocity was increased from about 15 cm/s to 21.4 cm/s, the mean F value decreased from 3.734 to 2.373. Even for the first three tests, it is seen from Table 2 that as the flow velocity was changed from 15.0 to 15.6 to 16.0 cm/s, the multiplying factor decreased from 3.885 to 3.756 to 3.560 respectively.

The larger calibration factor for slower flow was not because the change of the response of the instrument to the presence of frazil, nor the change of the frazil's characteristics because of the slower flow. It was observed during the experiments that when the flow was slow, the frazil flocs would have difficulty in passing through the sensor probe because of insufficient momentum possessed by the flocs. The slow pasage of the frazil flocs through the sensor probe meant that the flocs had a longer resident time in the probe and hence gave a higher measured concentration. During the experiments, it was observed that occasionally large flocs would even be caught by the probe and would only be dislodged if hit by other large oncoming flocs. Light tapping of the probe support by hand would greatly help to dislodge the tangled flocs. For this reason, during the experiments, the support of the sensor probe was constantly tapped. As the flow velocity increased, the frazil flocs possessed greater momentum and was seen passing through the sensor probe smoothly. Tapping of the support for the experiments of fast flows was not necessary.

The slow passage of frazil flocs through the sensor probe when the flow velocity was low was further aggravated by the large size and the thicker flocs of the slow flow. When the flow was slow, the turbulence level of the flow would also be low and the frazil crystals were able to agglomerate into bigger and thicker flocs. On the other hand, when the flow velocity was high, the higher turbulence of the flow caused the agglomeration to break up into smaller and more evenly

distributed flocs. The above can be seen from comparing Fig. 9, which is the frazil concentration recording of Test 4 obtained by playing back the tape-recorded signal to the instrument, with Fig. 7. It is seen from Table 1 that the two calibration tests (Tests 2 and 4) producing these two recordings had about the same rate of heat loss to the air so the concentration of frazil for the shown time period should be about the same. However, a comparison of these two recordings shows that the 16.0 cm/s flow produced larger and denser flocs than those produced by the 21.4 cm/s flow. The latter also exhibits much more even distribution of the frazil flocs and the fluctuation of frazil was also less as can be seen from the more evenly distributed counts shown on the margin of the strip chart. Since turbulence affects the agglomeration characteristics of frazil, any factor that affects turbulence therefore is also a potential factor in influencing the calibration factor.

It follows from the above that if the flow velocity is sufficiently high, an asymtoptic F value will be approached. This asymtoptic calibration factor will be the real calibration factor of the frazil instrument because of the anisotropy of the frazil crystals. From the performed experiments, it could be seen that this real calibration factor should be less than but close to the least calibration factor of 2.207 obtained from the experiments because it was observed during Test 5 that the frazil flocs experienced little resistance in passing through the sensor probe.

A turbulence dependent coefficient may be introduced to account for the turbulence effect on the calibration factor. In mathematical terms, this means writing

$$F = C_t Fr \tag{29}$$

Where Fr is the real calibration factor of the instrument because of frazil crystal anisotropy and C_t is the turbulence correction coefficient. If the real calibration factor Fr is approximately taken

as 2.2, then the value of C_t for the five experiments will be those as shown in Table 2. To accurately establish the value of Fr and the functional relationship between turbulence and C_t is beyond the scope of this paper. At this point, it will be sufficient to say that with a setup slightly improved over the setup reported in this paper, the value of Fr and the values of C_t over a reasonable range of flow and consequently turbulence conditions should be obtainable.

6.0 SUMMARY AND CONCLUSION

The development and calibration of the frazil instrument may be summarized as follows:

1. The proposed theory shows that the concentration of frazil in water can be measured by measuring $(R_s - R_r)/R_r$, where R_s is the electrical resistance of a sample of frazil laden water between two electrodes and R_r is the resistance of an identical sample of frazil free water.
2. An instrument was designed and constructed to measure the above parameter.
3. The newly developed instrument was laboratory tested and calibrated. The testing showed that the instrument performed satisfactorily.
4. Because of the non-isotropic shape of the frazil crystals which had not been taken into consideration in the theory and the sluggishness of the frazil flocs in passing through the sensor probe, the measured concentration of frazil was greater than the concentraion calculated from heat balance measurements by a calibration factor F.
5. F may be considered to be the product of two parts, the correction factor because of the anisotropy of the frazil crystals Fr and the corrective coefficient because of the sluggishness of the frazil flocs C_t.
6. At a high flow velocity of 21.4 cm/s during the laboratory testing, the frazil floc was observed to show little sluggishness in passing

through the sensor probe. The turbulence corrective coefficient C_t, therefore, should be approximately unity and the calibration factor F should be approximately equal to the corrective factor because of the non-isotropic shape of the frazil crystal Fr alone. This value of Fr, which is called the real calibration factor of the instrument, was found to be approximately 2.2.

7. At a slow flow velocity of 15-16 cm/s, the turbulence corrective coefficient was found to be in the range of 1.6-1.8. Further calibrations of the instrument will be needed to obtain the values of F or C_t under other flow and turbulence conditions.

ACKNOWLEDGEMENTS

The assistance of Mr. Manuel Pedrosa in designing and constructing the electronic hardware and the assistance of Mr. Paul Carney in designing and constructing the mechanical hardware are gratefully acknowledged.

REFERENCES

Ford, J.S. 1982. An Engineering Proposal for a Frazil Recorder. Technical Note No. E82-02, Hydraulics Division, National Water Research Institute, Burlington, Ontario, February.

Foulds, D.M. and T.E. Wigle. 1977. Frazil - The Invisible Strangler. Journal of American Waterwork Assoc., April, pp. 196-199.

Giffen, A.V. 1973. The Occurrance and Prevention of Frazil Ice Blockage at Water Supply Intakes. Research Report N43, Ministry of the Environment, Government of Ontario, 32 pp.

Giffilian, R.E., W.L. Line, and T. Osterkamp. 1972. Ice Formation in a Small Alaskan Stream, UNESCO-5: Properties and Process of River and Lake Ice.

Kristinsson, B. 1970. Ice Monitoring Equipment. Proceedings of IAHR Symp. on Ice and Its Action on Hydraulic Structures, Reyjavik, Sept., pp. 1.1-1-14.

Ontario Hydro. 1969. Study of River and Lake Ice - I.H.D. Project No. C 6.7, File Reference: R-SIG-6; Ontario - 27, Progress Report No. 3, Niagara River Ice, Sept., Contributors, Bryce, J.B., R.S. Arden and T.E. Wigle.

Schmidt, C.C. and J.R. Golver. 1975. A Frazil Ice Concentration Measuring System Using a Laser Doppler Velocimeter. Journal of Hydraulic Research, IAHR, Vol. 13, No. 3, pp. 299-314.

Tsang, G. 1973. Conceptual Design of a Multi-Purpose Instrument for Winter Stream Metering, Proceedings of Interdisciplinary Symp. on Advance Concepts and Techniques in the Study of Snow and Ice Resources, Monterey, California, Dec. 2-6, 1973, Proceedings published by National Academy of Sciences, Washington, D.C., 1974, pp. 688-698.

Tsang, G. 1977. Development of an Experimental Frazil Ice Instrument. Proc. of 3rd National Hydrotechnical Conf., Quebec, May, pp. 671-692.

Tsang, G. 1982a. Frazil and Anchor Ice - A Monograph, National Research Council of Canada Publ., February.

Tsang, G. 1982b. Resistance of Beauharnois Canal in Winter. Journal of the Hydraulics Div., ASCE, Vol. 108, No. HY 2, Feb., pp. 167-186.

Tsang, G. 1983. Formation and Properties of Frazil Formed in Seawater at Different Supercoolings. Proc. of Conf. of Port and Ocean Engineering under Arctic Conditions (POAC'83), Helsinki, April. Vol. 3, pp. 222-241.

Tsang, G. and T.O'D. Hanley. 1983. Frazil Formation in Water of Different Salinities and Supercoolings. Paper submitted to the Journal of Glaciology for possible publication.

LIST OF FIGURES

LIST OF TABLES

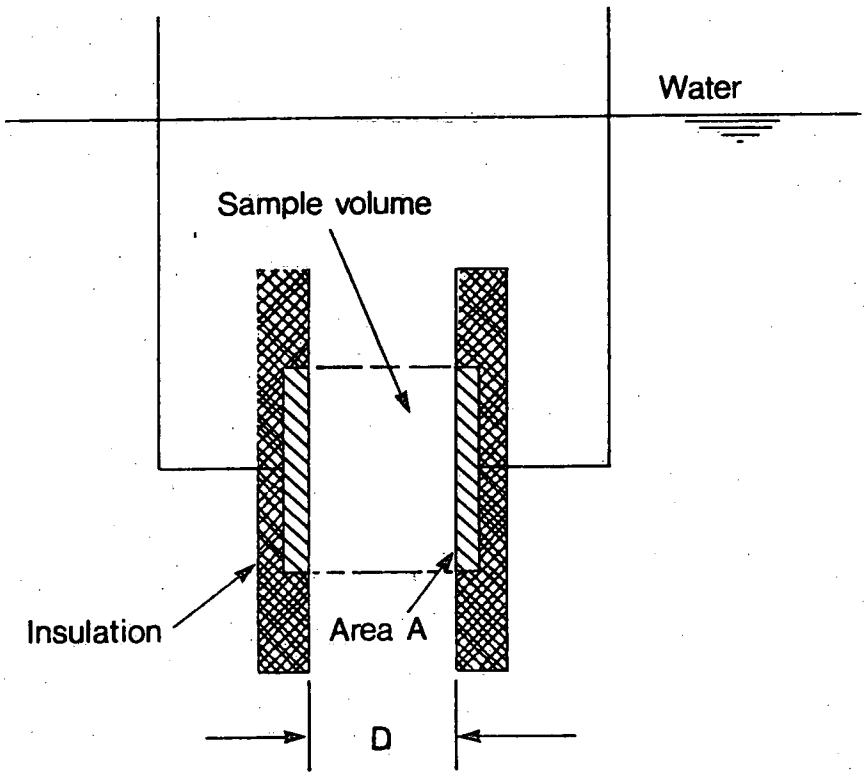

Fig. 1 Resistance between Two Insulated Plates

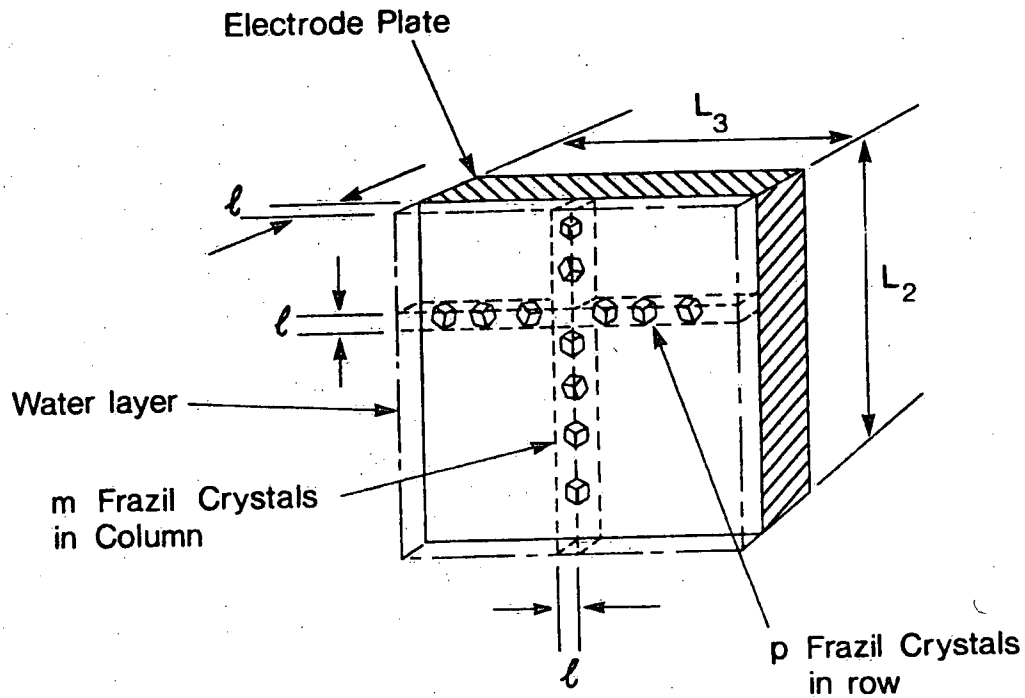

Fig. 2 Blockage of Electrical Line Receiving Area of Electrode Plate by Frazil Crystals.

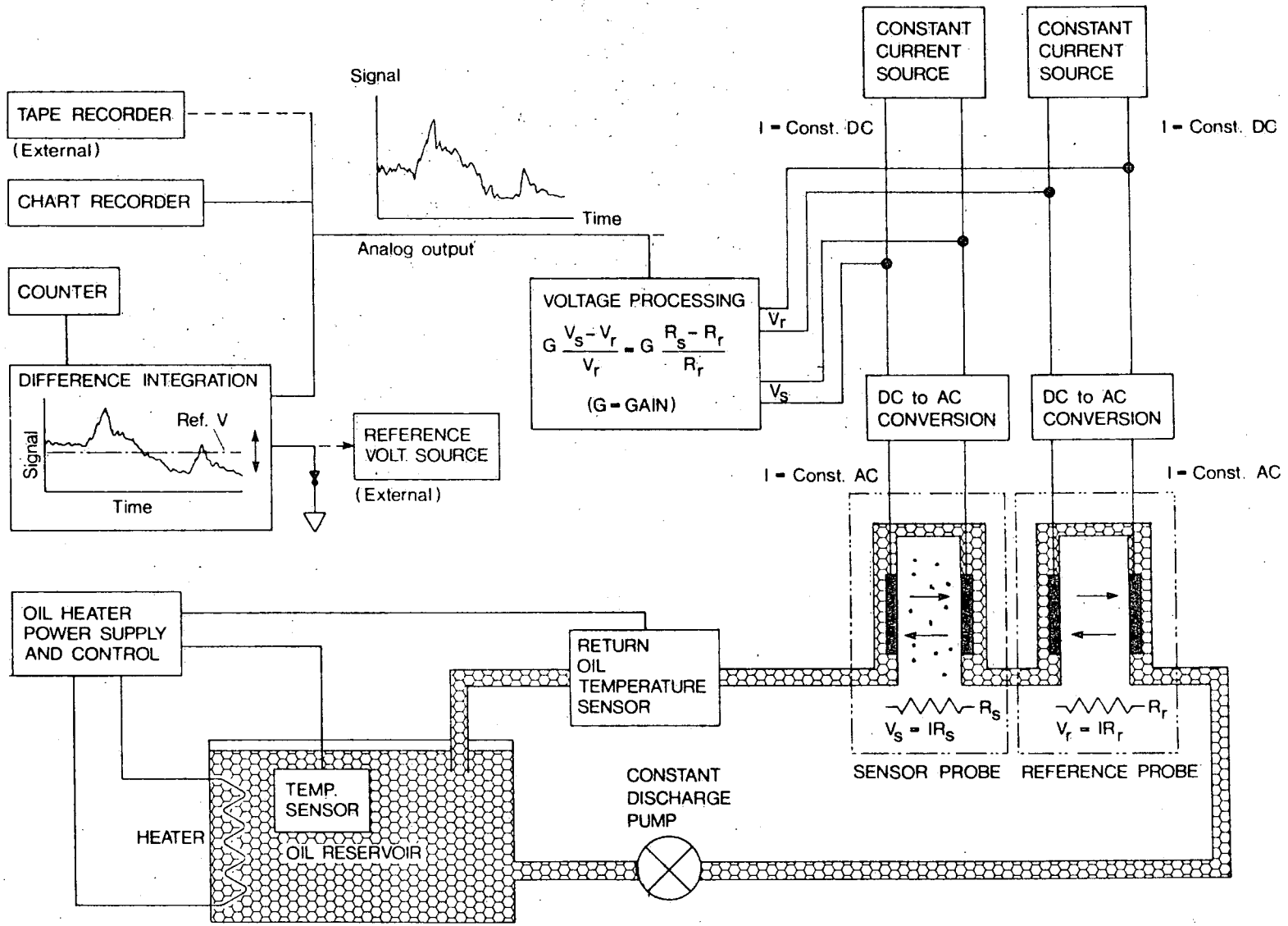

FIG. 3 CONCEPTUAL DESIGN OF FRAZIL INSTRUMENT

Fig. 4 Frazil Instrument for Laboratory Use

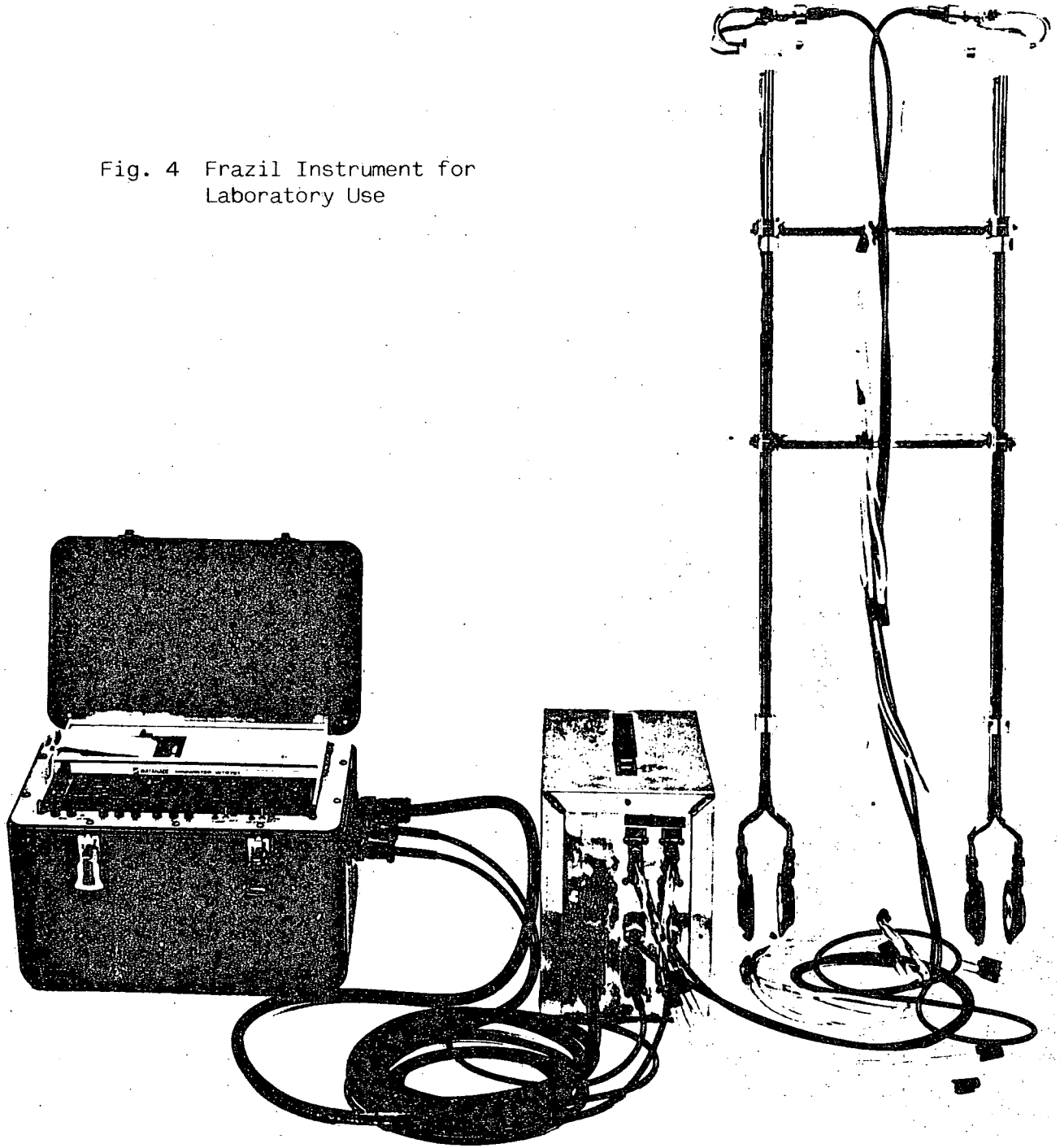

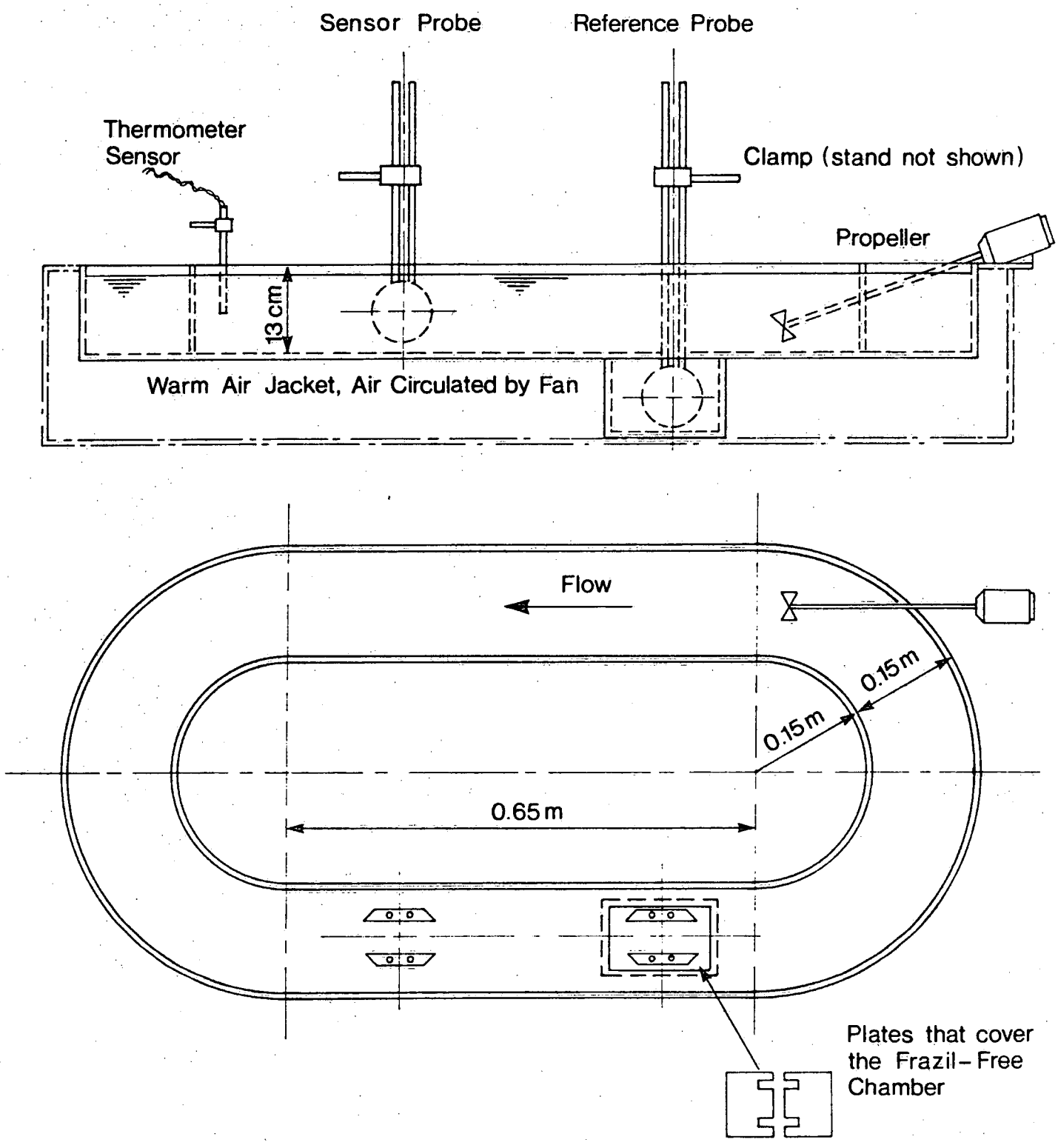

Fig. 5 Recirculating Flume and Calibration Setup

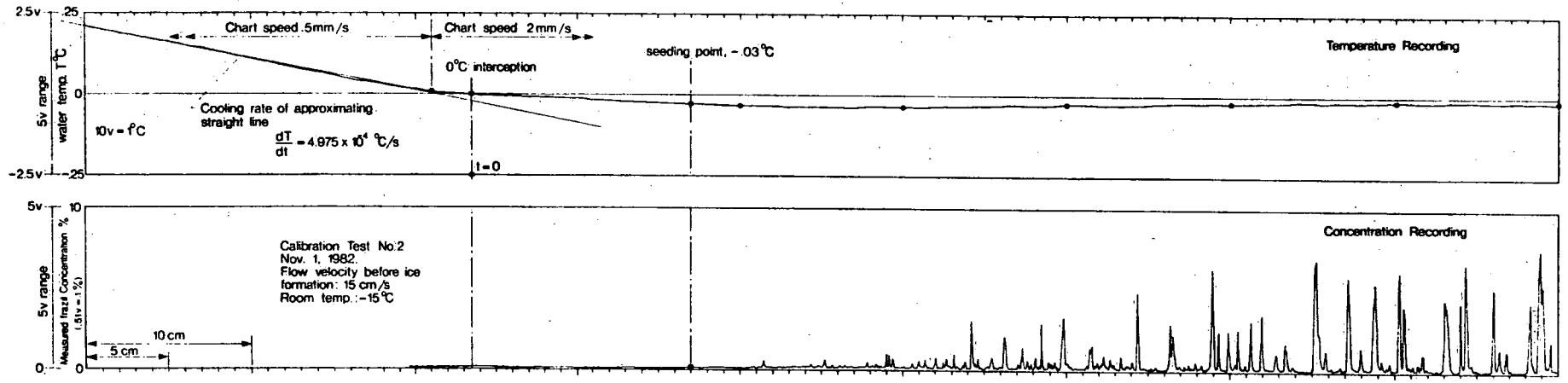

Fig. 6 Experimental Recording of Early Part of Test 2.

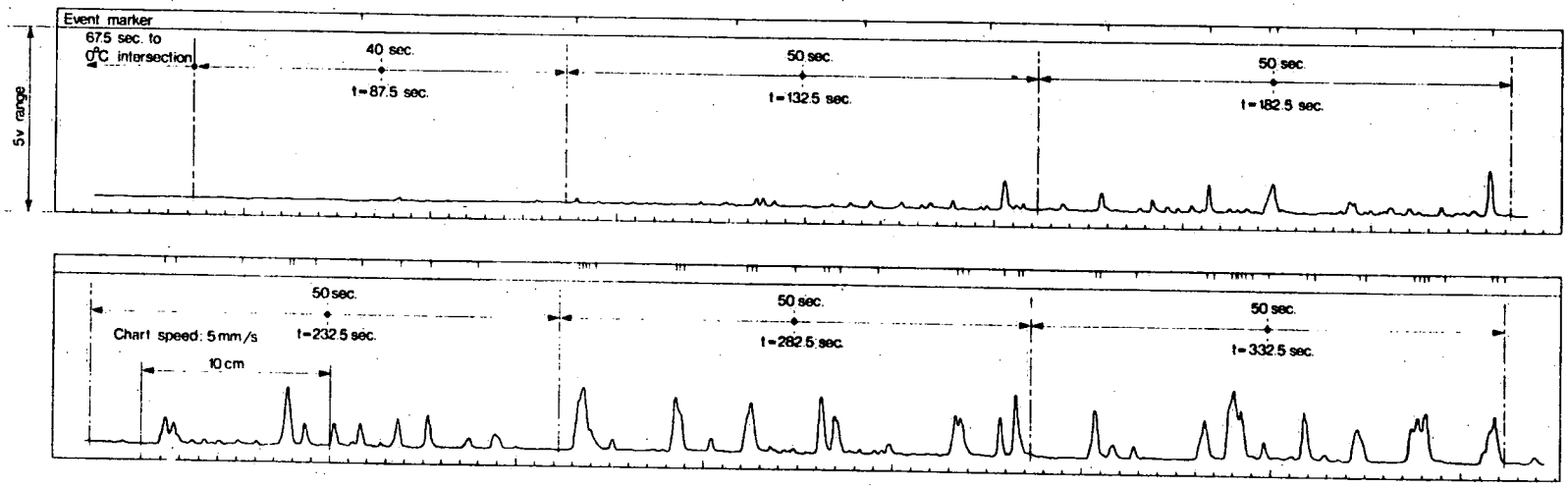

Fig. 7 Frazil Concentration Recording of Test 2 with Average Concentration Counts Shown on Margin (0.255 V = 1 % Frazil).

Fig. 8 Calibration Relationship of Instrument

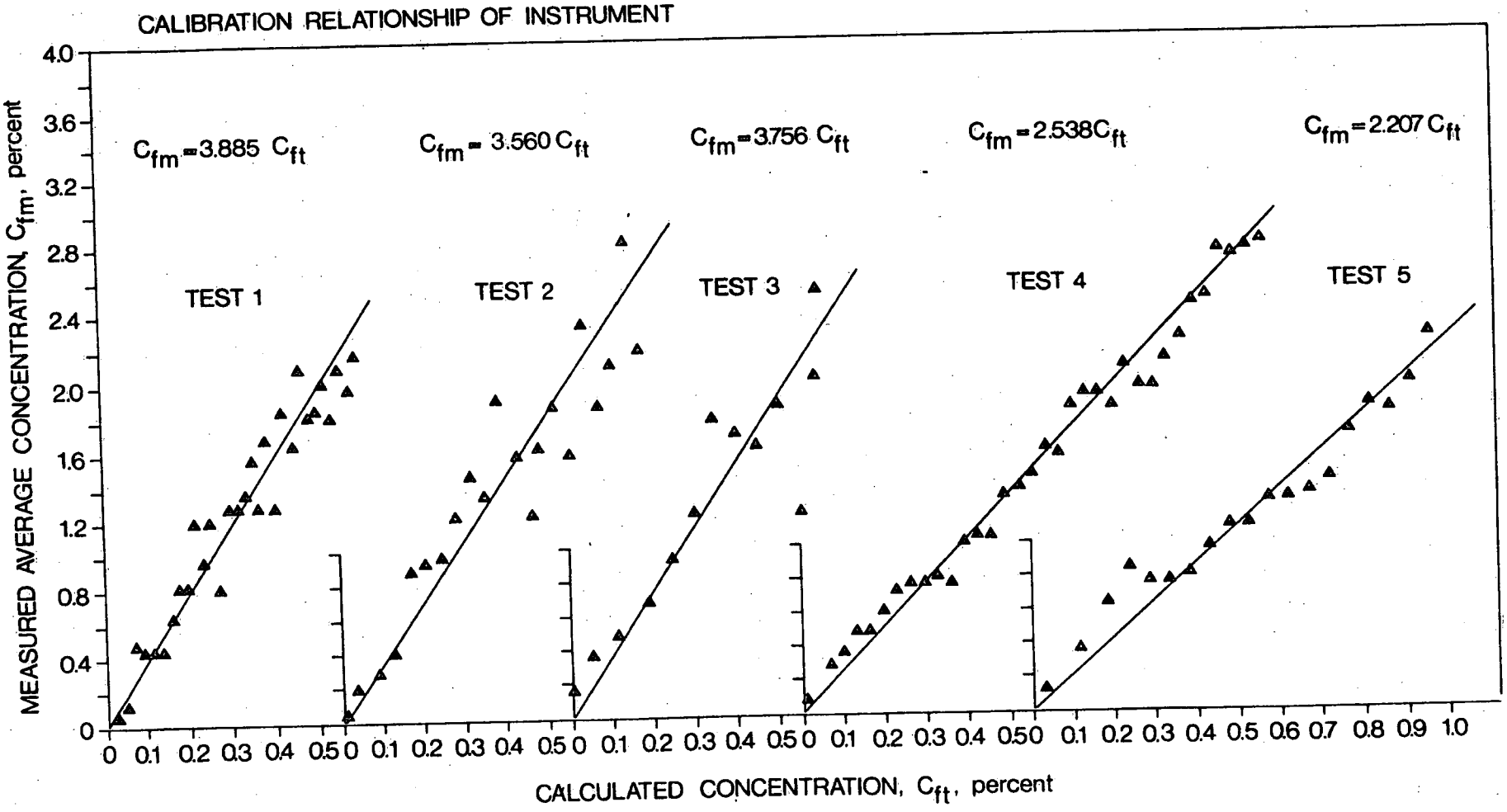

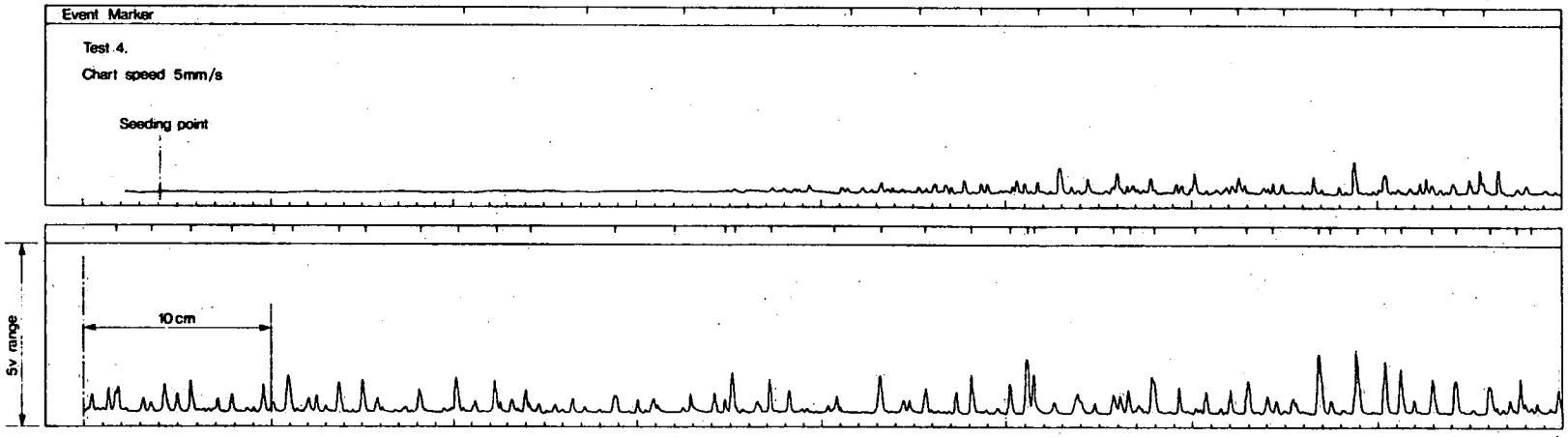

Fig. 9 Frazil Concentration Recording of Test 4 with Average Concentration Counts Shown on Margin (0.255 V = 1 % Frazil).

TABLE 1. SUMMARY OF CALIBRATION EXPERIMENTS

Test No.	1	2	3	4	5
Flow Velocity before Ice V cm/s	15.0	16.0	15.6	21.4	21.4
Air Temperature T_a °C	-10	-15	-20	-15	-20
Cooling Rate of Water at Seeding $(dT/dt)_n$ 10^{-4} °C/s	2.707	4.975	7.350	4.670	6.848
Seeding Temperature T_n °C	-.030	-.030	-.030	-.030	Spontaneous Nucleation
Conductivity of Water ρ μmho/cm	210	-	285	263	200

Time from 0°C t sec.	Calc. Concent. c_{ft} %	Measured Conc. c_{fm} %	t	c_{ft}	c_{fm}	t	c_{ft}	c_{fm}	t	c_{ft}	c_{fm}	t	c_{ft}	c_{fm}
121.5	0.000	0.00	67.5	0.000	0.00	42.0	0.000	0.00	65.0	0.000	0.00	67.0	0.000	0.00
191.5	0.023	0.06	87.5	0.009	0.04	67.5	0.003	0.16	95.0	0.011	0.08	117.0	0.027	0.12
241.5	0.047	0.12	132.5	0.035	0.20	117.5	0.054	0.36	145.0	0.068	0.28	167.0	0.110	0.36
291.5	0.072	0.48	182.5	0.086	0.28	167.5	0.112	0.48	195.0	0.099	0.36	217.0	0.178	0.64
341.5	0.092	0.44	232.5	0.127	0.40	217.5	0.190	0.68	245.0	0.130	0.48	267.0	0.232	0.84
391.5	0.115	0.44	282.5	0.170	0.88	267.5	0.247	0.92	295.0	0.161	0.48	317.0	0.280	0.76
441.5	0.135	0.44	332.5	0.206	0.92	317.5	0.302	1.20	345.0	0.193	0.60	367.0	0.327	0.76
491.5	0.158	0.64	382.5	0.246	0.96	367.5	0.351	1.76	395.0	0.227	0.72	417.0	0.373	0.80
541.5	0.178	0.82	432.5	0.280	1.20	417.5	0.405	1.68	445.0	0.261	0.76	467.0	0.422	0.96
591.5	0.197	0.82	482.5	0.314	1.44	467.5	0.451	1.60	495.0	0.294	0.76	517.0	0.468	1.08
641.5	0.215	1.20	532.5	0.349	1.32	517.5	0.503	1.84	545.0	0.325	0.80	567.0	0.513	1.08
691.5	0.234	0.96	582.5	0.383	1.88	567.5	0.556	1.20	595.0	0.358	0.76	617.0	0.561	1.24
741.5	0.252	1.20	632.5	0.429	1.56	607.5	0.593	2.00	645.0	0.390	1.00	667.0	0.608	1.24
791.5	0.272	0.80	682.5	0.463	1.20	672.5	0.598	2.50	695.0	0.422	1.04	717.0	0.655	1.28
841.5	0.296	1.28	732.5	0.484	1.60				745.0	0.453	1.04	767.0	0.703	1.36
891.5	0.315	1.28	782.5	0.519	1.84				795.0	0.485	1.28	817.0	0.751	1.64
941.5	0.334	1.36	832.5	0.558	1.56				845.0	0.520	1.32	867.0	0.798	1.80
991.5	0.352	1.56	882.5	0.593	2.32				895.0	0.555	1.40	917.0	0.846	1.76
1041.5	0.366	1.28	932.5	0.628	1.84				945.0	0.587	1.56	967.0	0.893	1.92
1091.5	0.385	1.68	982.5	0.658	2.08				995.0	0.618	1.52	1017.0	0.940	2.20
1141.5	0.404	1.28	1032.5	0.696	2.80				1045.0	0.649	1.80			
1191.5	0.424	1.84	1082.5	0.727	2.16				1095.0	0.680	1.88			
1241.5	0.447	1.64							1145.0	0.713	1.88			
1291.5	0.466	2.08							1195.0	0.746	1.80			
1341.5	0.484	1.80							1245.0	0.780	2.04			
1391.5	0.500	1.84							1295.0	0.812	1.92			
1441.5	0.518	2.00							1345.0	0.845	1.92			
1491.5	0.536	1.80							1395.0	0.875	2.08			
1541.5	0.554	2.08							1445.0	0.910	2.20			
1591.5	0.578	1.96							1495.0	0.940	2.40			
1641.5	0.595	2.16							1545.0	0.971	2.44			
									1595.0	1.002	2.72			
									1645.0	1.035	2.68			
									1695.0	1.068	2.72			
									1745.0	1.102	2.76			

Notes:
1. The temperature at which the conductivity of water was measured for Tests 1, 3, 4 and 5 was 6.0, 18.8, 12.0 and 5.0 °C respectively. The same water was used for both Tests 2 and 4.
2. The wind velocity over the flume was about 0.5 m/s.
3. For Test 5, frazil was observed before water temperature reaching -.030 °C.
4. The averaging time for calculating frazil concentration was 50 seconds for all tests.

Table 2. Calibration Coefficients of Instrument

Test No.	1	2	3	4	5
Flow velocity before ice, cm/s	15.0	16.0	15.6	21.4	21.4
Air temperature, ^{o}C	-10.0	-15.0	-20.0	-15.0	-20.0
Calibration factor, $F = c_{fm}/c_{ft}$	3.883	3.560	3.756	2.538	2.207
Average F		3.734		2.373	
Turbulence correction coefficient c_t	1.77	1.62	1.71	1.15	1.00

16091